Direct measurement of the apparent slip length

Pierre Joseph* and Patrick Tabeling

Laboratoire MMN, UMR CNRS-ESPCI 7083, 10 rue Vauquelin, F-75231 Paris Cedex 05, France
(Received 22 November 2004; published 31 March 2005)

We measure velocity profiles in water flowing through thin microchannels, using particle image velocimetry combined with a nanopositioning system. From the velocity profiles, we determine the slip lengths in two cases: Smooth hydrophilic glass surfaces, and smooth hydrophobic glass surfaces, grafted with a monolayer of silane. The slip length is determined within ($\pm$100 nm), i.e., five times more accurately than previous work. In all cases, we find that the slip length is below 100 nm.

The no-slip hydrodynamic boundary condition for liquids states that velocities on solid walls are zero. This postulate, consistent with decades of experimental work carried out with nonminiaturized systems, has recently been revised on the basis of experimental evidence. One central notion is this area is the slip length, which characterizes the amount of slip at the surface. Its definition is embodied in the Navier boundary condition which reads:

$$v_{z=z_w} = b \frac{\partial v}{\partial z},$$

where $v_{z=z_w}$ is the velocity at the wall, b is the extrapolation or slip length, and z is the normal at the wall inwards to the liquid. A series of experiments performed since 1999 brought detailed measurements of b [1–17]. As a whole, it appears that wetting liquids satisfy no-slip conditions on the boundaries. On the other hand, decreasing liquid-solid interactions (thus favoring nonwetting conditions) promotes large slip lengths. In the most extreme cases, slip lengths on the order of several microns for smooth hydrophobic surfaces were reported for a range of shear rates lying well below a molecular scale [2,12]. Although qualitately consistent with numerical studies, this set of measurements lies well above estimates based on direct numerical simulation for which slip lengths do not exceed thirty intermolecular scales, throughout a range of shear rates comparable to the experiment [18,19]. Further experimental effort carried out in 2002–2003 obtained lower slip lengths, raising issues concerning the robustness of large slip phenomena. Should the observations of Refs. [2,12] be confirmed, this would have considerable implications for the domain of microfluidics: This would open a pathway to obtaining a substantial reduction of the flow dissipation in channel of sizes comparable to b, along with decreasing Taylor dispersion, which acts as a limiting factor for miniaturized separation systems.

The observations of [2,11,12] challenged the theory. To date, the current theoretical hypothesis for accounting slip lengths reaching thousands of molecular scales bears on the existence of a gaseous film, lying between the wall and the liquid. Such a layer would generate a large apparent slip [20,21]. The presence of nanoscale gaseous structure has been shown experimentally beneath a hydrophobic wall and a liquid at rest, thus providing indirect support to the theoretical hypothesis [22,23].

In an effort to assess the experimental situation, we attempted to reproduce the measurements of Ref. [12]. Particle image velocimetry (PIV) technique deserves particular attention because it provides a direct access to the slip phenomenon. In our work, we obtain an unprecedented precision on the PIV slip length measurement. The main result of this communication is that the slip length we find is below 100 nm, an estimate closer to numerical findings, and much smaller than those reported in Ref. [12].

The experimental setup is shown in Fig. 1. The 10 μm $\times$ 100 μm $\times$ 1 cm microchannel is made in polydimethylsiloxane (PDMS), using a standard soft lithography tech-
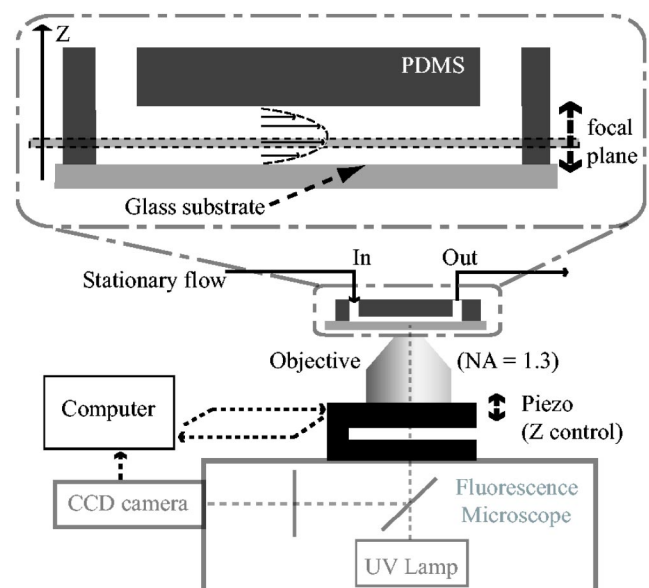
FIG. 1. Scheme of the experiment. A stationary flow of fluorescent tracers in deionized water is imposed in a PDMS/glass microchannel. The lower surface, a microscope coverslip, can be chemically modified before enclosure. The focal plane is controlled with a piezo, a large numerical aperture objective allowing a narrow depth of field. Velocity is measured by particle image velocimetry. The entire velocity profile is determined thanks to a scan on z position.

*Electronic mail: pierre.joseph@espci.fr; www.mmn.espci.fr
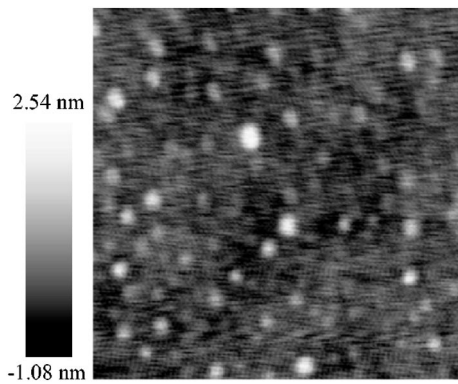
FIG. 2. 500 nm×500 nm tapping mode AFM image of a hydrophobic surface (OTS grafted on glass). rms roughness is 0.45 nm. This surface is the one used in measurements of Fig. 4(b).

FIG. 3. Determination of the wall position: Averaged intensity of each adsorbed particle is fitted with a Lorentzian. The particle radius is removed to the mean z position of the peaks to give the actual glass location within ±30 nm.

nique. The lower boundary is a microscope glass coverslip, whose roughness and wetting properties are controlled. We worked with hydrophilic bare glass and hydrophobic grafted glass. In the hydrophilic case, the roughness measured by atomic force microscopy (AFM) technique prior to closing the channel is less than 0.5 nm root-mean square (rms). Hydrophobic surfaces are obtained by coating the glass with hydrophobic monolayers of silanes, either octadecyltrichlorosilane (OTS) or chlorodimethyloctylsilane (CDOS). Grafting is achieved in anhydrous toluene, after cleaning and activating the surface with an oxygen plasma. The contact angle of water on the prepared surface is 95°, with less than 10° hysteresis between advancing and receding angles. Tapping-mode AFM images reveal a rms roughness of about 0.45 nm (see Fig. 2). The flowrate is set by controlling the inlet and outlet pressures. The pressure drop along the channel is lower than 5 mbar, the outlet being held at atmospheric pressure. The working solution is deionized water seeded with fluorescent particles, 10^{-5} in volumetric concentration. Velocity is measured by micro-particle image velocimetry, a technique which is now well documented [24]. Briefly, it consists in tracking the peaks of the intensity cross correlation of a cell, at two different times. In our case, the cell dimensions are 12 μm×25 μm and the time separation is 20 ms. The results are further averaged over 25 pairs of images. The velocity histograms are symmetric with respect to their mean, so the choice of the average process shows no visible influence on the result. The fluorescent beads we used have diameters equal to 100 or 200 nm. These sizes yield an acceptable spatial resolution for the velocity measurements; on the other hand, the tracers are large enough to be little affected by brownian motion. Brownian diffusion not only adds noise to the measurement, but may also let some particles exit the focal plane between two successive images, decreasing the locality of the measurement. As a whole, it results in a few percent noise in the velocity measurement; this level is reduced below 1% by averaging. Close to the solid, the particles develop hydrodynamic interaction with the walls, and their trajectories cease to be those of the fluid. At the low Reynolds numbers investigated here, this effect can be quantified [25]. The tracers velocity is that of the fluid within less than 1% for distances from the wall larger than
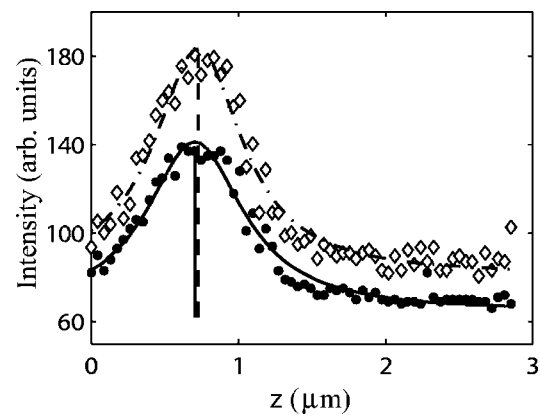
three particle radius, a condition verified for all beads in our system (see discussion below). In addition, it was recently stressed that the streaming electric field induces the electrophoresis of the beads, which may lead to an apparent slip length for the tracers, even though the solvent verifies the no-slip boundary condition [26]. For our case—zeta potential measured to be 50 mV and 100 mV for the particles and the wall, respectively, Debye length λ_d=100 nm—the error introduced on the slip length is inferior to 10 nm.

The observation is made with a charge coupled device (CCD) camera coupled to a LEICA epifluorescent microscope, with a 100× oil immersion large numerical aperture objective (NA=1.3), which depth of field is 700 nm. The microscope objective is mounted onto a piezotransducer. The location of the focal plane in the vertical axis (z) is known with a 10 nm *relative* precision. Owing to the fact that the ray crosses different optical medias, the actual z position of the focal plane is: $z=(n_w/n_{oil})z_p$, where z_p is the piezoposition, n_w and n_{oil} oil and water index of refraction. A scan on z axis with 50 nm step increments is realized from the bottom (glass wall) to the top (PDMS wall) of the channel, so as to entirely determine the velocity profile $v(z)$ across the channel. By thresholding on the intensity and then selecting the particles in focus, the optical depth of the PIV volume is Δz=500 nm; we thus obtain an imaged zone defined as a 500 nm×12 μm×25 μm parallelepiped. By assuming uniform bead concentration, and noting the flow is uniform in the horizontal plane, the actual velocity we measure at a fixed z represents the average velocity over the probing volume.

In order to determine the slip length, it is crucial to accurately determine the wall position. This is done by taking advantage of the presence of a few particles, unavoidably adsorbed onto the lower wall. The window of observation is consequently chosen to include two or three such beads. The intensity emitted by each of them is plotted on Fig. 3. By fitting such a curve with a Lorentzian (see Fig. 3)—a function representing the intensity distribution around a local source [27]—and substracting the bead radius, the wall location is determined within 30 nm.
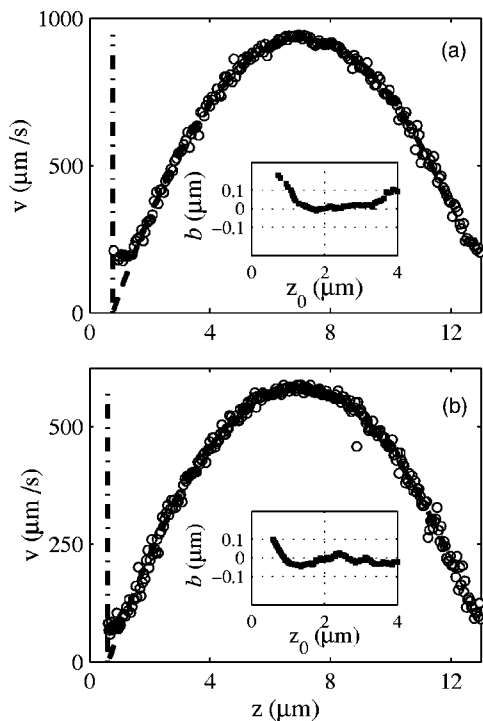
FIG. 4. (a) Velocity profile and parabolic fit for a smooth and hydrophilic substrate (glass). The dashed-dotted line shows the position of the solid wall. The inset corresponds to the variation of the slip length when changing the origin z_0 of the fit zone, for a fixed end $z_f = 12$ μm. (b) Averaged velocity and parabolic fit for a hydrophobic monolayer of silane (OTS) grafted on glass.

FIG. 5. Slip length b as a function of the shear rate at the wall, for water flowing on different surfaces: (a) hydrophilic glass and (b) hydrophobic monolayers of OTS on glass (white circles) and CDOS on glass (black diamonds).

Typical velocity profiles obtained for hydrophilic and hydrophobic substrates are shown in Fig. 4. Measurements performed at a distance from the wall inferior to $\Delta z/2$ have been corrected to take into account the fact that the probing volume incorporates wall regions, where there is no particle. One obtains a parabolic profile, with a protuding foot within the first hundreds nanometers from the walls. It originates from the electrostatic repulsion between the particles and the wall. The beads are depleted at a minimum distance from the wall of about 300 nm, which prevents particles and substrate Debye layer to overlap, as discussed in Ref. [28]. The minimum velocity one may measure by micro-PIV is that holding at that distance—hydrodynamics within the electric double layer on slipping surfaces, not investigated here, is discussed in Ref. [29]. Data outside this region are not perturbed by these effects, and do represent actual fluid velocities. We thus fit such Poiseuille-type profiles with a parabola: The slip length b is the difference between the measured position of the wall and the extrapolation of this parabola to zero. The fit is realized for different measurement windows. In the insets of Fig. 4, we keep the end of the window constant ($z_f = 12$ μm), and shift its origin, on the left side, from $z_0 = z_w$ (the wall position) to 4 μm. One finds that b levels off at a well defined value for $z_0 - z_w > 500$ nm. This observation is consistent with the fact that PIV measurements tend to be perturbed close to the wall, as discussed previously. The value of z_f (the end of the window used for the fit) shows no influence on the mean value of the plateau, as long as mea-

surements near the PDMS wall (where electrostatic and hydrodynamic effects similar to those discussed for the glass substrate occur) are not included. The asymptotic value of b is taken as the slip length.

A summary of the slip length measurements using hydrophilic glass is shown in Fig. 5(a), where b is plotted as a function of the shear rate $\dot{\gamma}_w$ at the wall. With an average value $b = 50$ nm, and a standard deviation 50 nm, these results indicate that the slip length of water on a smooth glass surface is inferior to 100 nm, consistently with a number of studies performed with similar systems [1,12]. The results for smooth hydrophobic surfaces are shown in Fig. 5(b) for OTS (white circles) and CDOS (black diamonds) on glass. The measured slip lengths for these two systems show no dependence on the shear rate, the average values are $b = -35 \pm 100$ nm for OTS and $b = 57 \pm 100$ nm for CDOS. The main result is then that there is no huge slip effect for water flows on hydrophobic and smooth substrates. One may recall that the range of shear rates at the wall investigated here (up to $\dot{\gamma}_w = 450$ s^{-1}) is comparable to that used by Tretheway and Meinhart [12], who measured the apparent slip length of water equal to 1 μm ± 450 nm, on a monolayer of silane similar to ours—roughness and contact angle measured on a reference section to be respectively 3 Å and 120°. The discrepancy between the two measurements underlines the difficulty to obtain large slips in a robust way. Further progress on the subject may probably rest on the detailed

investigation of possible gaseous structure in the first tens of nanometers from the wall. From a practical viewpoint, our results indicate that it is uncertain to rely on the sole presence of smooth hydrophobic surfaces to obtain large slips in microfluidic systems. A more reliable approach could be micropatterning the surfaces so as to sustain permanent gaseous structures, as suggested in recent numerical studies [30] and experiments [31].

[1] C. Cottin-Bizonne, S. Jurine, J. Baudry, J. Crassous, F. Restagno, and E. Charlaix, Eur. Phys. J. E **9**, 47 (2002).

[2] Y. Zhu and S. Granick, Phys. Rev. Lett. **87**, 096105 (2001).

[3] Y. Zhu and S. Granick, Phys. Rev. Lett. **88**, 106102 (2002).

[4] V. S. J. Craig, C. Neto, and D. R. M. Williams, Phys. Rev. Lett. **87**, 054504 (2001).

[5] E. Bonaccurso, M. Kappl, and H.-J. Butt, Phys. Rev. Lett. **88**, 076103 (2002).

[6] E. Bonaccurso, H.-J. Butt, and V. S. J. Craig, Phys. Rev. Lett. **90**, 144501 (2003).

[7] C.-H. Choi, K. J. A. Westin, and K. S. Breuer, Phys. Fluids **15**, 2897 (2003).

[8] S. Jin, P. Huang, J. Park, J. Yoo, and K. Breuer, Exp. Fluids **37**, 825 (2004).

[9] K. Watanabe, Y. Udagawa, and H. Udagawa, J. Fluid Mech. **381**, 225 (1999).

[10] J.-T. Cheng and N. Giordano, Phys. Rev. E **65**, 031206 (2002).

[11] R. Pit, H. Hervet, and L. Leger, Phys. Rev. Lett. **85**, 980 (2000).

[12] D. C. Tretheway and C. D. Meinhart, Phys. Fluids **14**, L9 (2002).

[13] J. Baudry, E. Charlaix, A. Tonck, and D. Mazuyer, Langmuir **17**, 5232 (2001).

[14] C. Cheikh and G. Koper, Phys. Rev. Lett. **91**, 156102 (2003).

[15] J.-H. J. Cho, B. M. Law, and F. Rieutord, Phys. Rev. Lett. **92**, 166102 (2004).

[16] C. Henry, C. Neto, D. R. Evans, S. Biggs, and V. S. J. Craig, Physica A **339**, 60 (2004).

[17] C. Cottin-Bizonne, B. Cross, A. Steinberger, and E. Charlaix, Phys. Rev. Lett. **94**, 056102 (2005).

[18] J.-L. Barrat and L. Bocquet, Phys. Rev. Lett. **82**, 4671 (1999).

[19] P. A. Thompson and S. M. Troian, Nature (London) **389**, 360 (1997).

[20] P.-G. de Gennes, Langmuir **18**, 3413 (2002).

[21] D. Andrienko, B. Dünweg, and O. I. Vinogradova, J. Chem. Phys. **119**, 13106 (2003).

[22] J. W. G. Tyrrell and P. Attard, Phys. Rev. Lett. **87**, 176104 (2001).

[23] T. R. Jensen, M. Ø. Jensen, N. Reitzel, K. Balashev, G. H. Peters, K. Kjaer, and T. Bjørnholm, Phys. Rev. Lett. **90**, 086101 (2003).

[24] J. G. Santiago, S. T. Wereley, C. D. Meinhart, D. J. Beebe, and R. J. Adrian, Exp. Fluids **25**, 316 (1998).

[25] A. J. Goldman, R. G. Cox, and H. Brenner, Chem. Eng. Sci. **22**, 653 (1967).

[26] E. Lauga, Langmuir **20**, 8924 (2004).

[27] M. G. Olsen and R. J. Adrian, Exp. Fluids **29**, S166 (2000).

[28] D. Lumma, A. Best, A. Gansen, F. Feuillebois, J. O. Rädler, and O. I. Vinogradova, Phys. Rev. E **67**, 056313 (2003).

[29] L. Joly, C. Ybert, E. Trizac, and L. Bocquet, Phys. Rev. Lett. **93**, 257805 (2004).

[30] C. Cottin-Bizonne, J.-L. Barrat, L. Bocquet, and E. Charlaix, Nat. Mater. **2**, 237 (2003).

[31] J. Ou, B. Perot, and J. P. Rothstein, Phys. Fluids **16**, 4635 (2004).